Journal of Organometallic Chemistry 693 (2008) 2021–2032

Contents lists available at ScienceDirect

Journal of Organometallic Chemistry

journal homepage: www.elsevier.com/locate/jorganchem

Synthesis and evaluation of thermal, photophysical and magnetic properties of novel starlike fullerene–organosilane macromolecules

Rachana Singh, Thakohari Goswami *

Electronics and Smart Materials Division, Defence Materials and Stores Research and Development Establishment, DMSRDE P.O., G.T. Road, Kanpur 208 013, India

ARTICLE INFO

Article history:
Received 30 December 2007
Received in revised form 29 February 2008
Accepted 6 March 2008
Available online 18 March 2008

Keywords:
Organo-silane fullerene derivatives
Functionalized fullerenol
Fullerene core starlike macromolecules
Magnetic properties
Photophysical properties

ABSTRACT

Thermal, photophysical and magnetic properties of some novel fullerenol–silane adducts are described. Excellent improvement of thermal stability and high char yield due to the presence of silicon is the key feature of these adducts. Highest luminescence quenching due to maximum π–π electronic interactions between phenyl ring and fullerene are observed in the aromatic-silane adducts and the quenching ability of the aromatic ring reduces with further delocalization of the π-electrons as in naphthyl silane. The alkyl vinyl silane, on the other hand, records better fluorescence intensity owing to increase population of the electron density (+I effect) and non-effective charge transfer complex formation between isolated vinylic double bond and fullerene. Emission peak positions of these adducts are comparable to fullerenol because of control derivatization of fullerene ring causing less perturbation of the symmetric π-electronic system. These adducts are paramagnetic in nature with peaks around 3515 G and higher *g*-values (2.005–2.009) compared to fullerenol (1.985). The fullerenol–silane adducts are synthesized using fullerenol as substrate and different chloro and alkoxy silanes as silylating agents adopting simple nucleophilic displacement and transesterification reactions. All the fullerenol–silane adducts are characterized spectroscopically.

1. Introduction

Silicon is the second most abundant element on the surface of the earth after oxygen and mildest of metals. The silicon compound that contains at least one carbon–silicon bond (R–Si) in the structure is known as organosilane. The non-polar silicon–carbon bond is very stable, and gives rise to low surface energy and hydrophobic effects [1–3]. Polysiloxanes have good oxidative stability, low surface energies, excellent biocompatibility, low glass transition temperature, good thermal stability. The combination of fullerene and polysiloxane can therefore promises to deliver novel material with unique properties that have wide potential for technological applications [4]. A series of linear polysiloxane anchored fullerene has been successfully prepared and is used as stationary phase for capillary gas chromatography [5–8]. A novel polysiloxane with pendant C_{60} and carbazole moieties is also being reported and the polymer possess good solubility, processability, film forming ability and photo-physical properties [9].

Covalent linking of silicon alkoxide end group of triethoxysilyl fulleropyrrolidine, other fulleropyrrolidines [10,11] and trialkoxysilyl functionalized fullerenes to hybrid organic/inorganic sol–gel network of silica glasses show better optical limiting behavior [12–19]. Attachment of [60]fullerene to poly(dimethylsiloxanes) using *o*-xylene derivatization method [20–25] leads to soluble and structurally defined fullerene-containing polymers. These materials exhibit high thermal stability and excellent film-forming properties [26]. The hydrosilylation of [60]fullerene with the poly(methyl hydrido methyloctyl siloxane) also produced a soluble antioxidant fullerene–siloxane copolymer [27]. The silylated fullerenes exhibit lower oxidation potentials than the parent fullerenes indicating that silylation effectively produce the electronegative fullerene derivatives. These silicon derivatives constitute an important stepping-stone towards the development of material for catalytic and biological applications [28].

The fullerenols [$C_{60}(OH)_n$] are interesting material and have drawn extensive attention because of their promising applications in many fields, viz, solar energy conservation and storage [29], fuel cells [30,31], macromolecular materials [32,33] and biomedical and life sciences [34,35]. The gadolinium fullerenols are reported to be the best candidate for new generation novel magnetic resonance imaging (MRI) contrast agent [36,37]. The advantage of high solubility, poly-ol functionality and ball shaped structure in fullerenol enriches its utilization as a spherical molecular core in the design of dendritic [38–40], and star-shaped macromolecules and polymers [41–48]. Chiang et al. [49] have synthesized soluble urethane-connected polyether star-like polymeric material containing six chemically bonded polymers arms per C_{60} (polydispersity index of 1.45) utilizing fullerenol as a molecular core. Incorporation of polyhydroxylated fullerene in the poly(urethane-ether)

* Corresponding author. Tel.: +91 512 2451758 71; fax: +91 512 2451740 40.
E-mail address: thgoswami@yahoo.co.uk (T. Goswami).

0022-328X/$ - see front matter © 2008 Elsevier B.V. All rights reserved.
doi:10.1016/j.jorganchem.2008.03.006

network gives high performance elastomers with greatly enhanced tensile strength, elongation, and thermo-mechanical stability in comparison to their linear analogs or conventional polyurethane elastomers cross-linked by tri-hydroxylated reagents [50]. A water soluble fullerene containing poly(ethylene oxide) (PEO) derivative is synthesized by the reaction of fullerenol with PEO having isocyanate groups [$MeO(CH_2CH_2O)_nCONH(CH_2)_6NCO$] in presence of dibutyl-tin dilaurate catalyst [51].

The strong electrophilic property of fullerene cage easily release protons to generate fulleroxide anion $(Fol–O)^{n-}$ and thus provide new family of proton conductors. The fulleroxide anion $(Fol–O)^{n-}$ is capable of undergoing selective nucleophilic addition reactions to carbonyl compounds in alkaline medium [47,52] and Michael addition reaction with α,β-unsaturated esters in both acid and alkaline condition [48,53,54]. The transesterification reaction of functionalized propyl-trialkoxy silane of the type $(RO)_3Si(CH_2)X$ (R = Me, X = Cl; R = Et, X = NH_2) with fullerenols is also reported [55]. Fullerenol undergoes nucleophilic substitution reaction with chlorodiphenyl phosphine forming poly-diphenylphosphite [60]fullerene ligand [55]. This ligand is highly reactive towards different metal compounds to form metal complexes. Fullerene bearing tertiary phosphine and P-chiral phosphonites are also synthesized and are used to form Pt(III) and Pd(II) metal complexes [56].

Fullerene hydroxyl groups form hydrogen bonds with pyridine nitrogen to develop fullerenol-poly (styrene-co-4-pyridine) nanocomposite. The nano-composite shows much higher storage modulus and better optical limiting performance [57]. A series of supramolecular assembled Fol-PDMS [poly(dimethoxy silane)] nanocomposites with controlled size fullerenol-nanodomains embedded in the PDMS matrix have been prepared [58]. Benefiting from the unique chiral structure and dielectric property of fol molecules, the resultant nanocomposites exhibit superior thermal and thermo-mechanical response and unique dielectric properties. The higher content of fol in the nanocomposites increases the permittivity but dramatically decreases the loss factor. Similar studies are also performed on to the fullerenol–polyurethane blends [45].

In the present article we describe the synthesis, characterization and property evaluation of some novel fullerene core starlike alkyl-phenyl/vinyl silane macromolecules. The fullerenol is used as substrate and different chloro silanes and alkoxy silanes are used as silylating agents. Displacement reaction of chlorosilanes and transesterification reaction of alkoxy silanes are two synthetic strategies adopted for the present work. Displacement reaction is carried out under inert atmosphere using DMF solution of fullerenol and triethyl amine as the chlorine scavenger. The fullerenol–silane adducts are highly soluble in DMSO. Evaluation of thermal, photophysical and magnetic properties of these materials suggest that these materials have potential for useful application in electroluminescent devices.

2. Results and discussion

2.1. Synthesis

Two different synthetic strategies are adopted for silylation. Schemes 1 and 2 present the procedure adopted for the displacement reaction of chlorosilane and transesterification reaction of alkoxy silane respectively. Triethyl amine is used as catalyst and acid (HCl) scavenger in displacement reaction of chlorosilane. The transesterification reaction of alkoxysilane reaction, on the other hand, is carried out without any catalyst. The typical chlorosilanes (**1**–**3**) and alkoxy silanes (**4** and **5**) used as silylating agents and their corresponding silane adduct of fullerenol (**1a**–**5a**) are presented in Schemes 1 and 2, respectively.

2.2. Synthesis of fullerenol

The fullerenol used in the present investigation is synthesized by the modified reported method [59]. It has been observed that the same reagents can produce different fullerenol isomers under suitable reaction conditions [60]. In a typical reaction 0.15 g NaOH (in 10 mL) is reacted with 100 mg of fullerene (in 100 mL toluene) for 2 h in presence of TBAH as phase transfer catalyst. The black

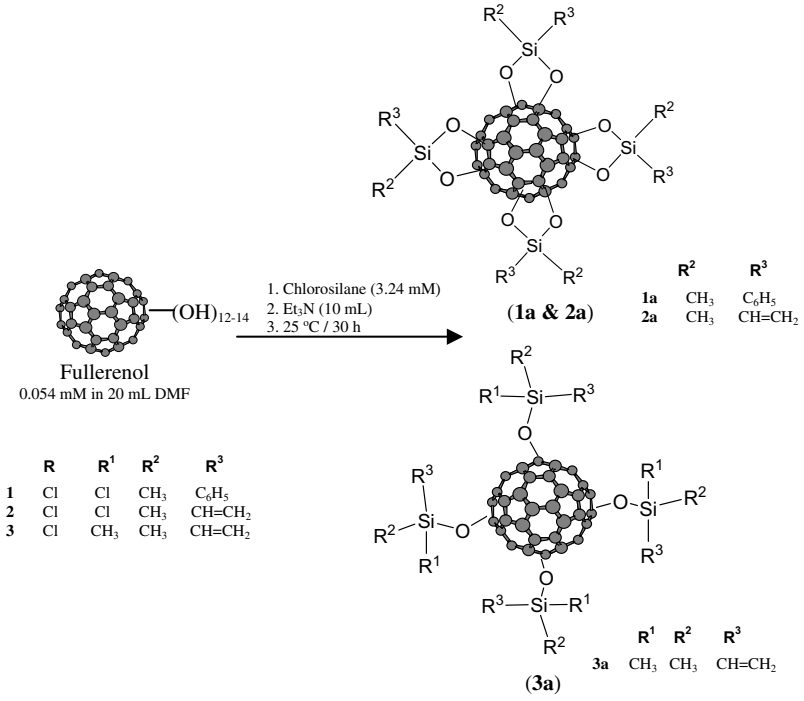

	R	R^1	R^2	R^3
1	Cl	Cl	CH_3	C_6H_5
2	Cl	Cl	CH_3	$CH=CH_2$
3	Cl	CH_3	CH_3	$CH=CH_2$

	R^2	R^3
1a	CH_3	C_6H_5
2a	CH_3	$CH=CH_2$

	R^1	R^2	R^3
3a	CH_3	CH_3	$CH=CH_2$

Scheme 1. Schematic representation of nucleophilic displacement reaction of chlorosilane with fullerenol.

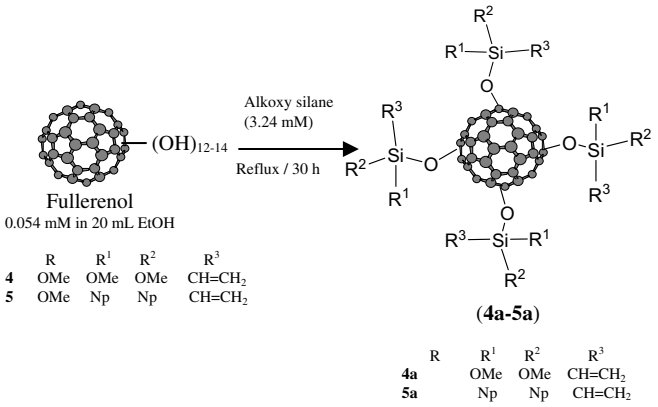

	R	R^1	R^2	R^3
4	OMe	OMe	OMe	$CH{=}CH_2$
5	OMe	Np	Np	$CH{=}CH_2$

	R	R^1	R^2	R^3
4a		OMe	OMe	$CH{=}CH_2$
5a		Np	Np	$CH{=}CH_2$

Scheme 2. Schematic representation of transesterification reaction of alkoxyosilane with fullerenol.

sludge, thus obtained, is first washed with methanol and subsequently with toluene to remove unreacted sodium hydroxide, TBAH and fullerene respectively. After drying the residue under vacuum, the dried solid is further washed with water to remove the water soluble fullerenol. The residual fullerenol is estimated to have 12–14 hydroxyl groups per fullerene [60].

2.2.1. Displacement reaction of chlorosilane (Scheme 1)

The reaction of chlorosilanes (**1**–**3**) with fullerenol is carried out in dry DMF solution using excess of triethyl amine as catalyst. In a typical reaction 0.05 g (0.054 mM) of fullerenol is suspended in dry-degassed DMF (20 mL). Triethyl amine in excess (10 mL) is added and mixed solution is cooled to −5 °C. Chlorosilane (3.24 mM) is then added at such a rate that the temperature of the reaction mixture never rise above 0 °C during entire addition. The initial reaction is highly exothermic and the reaction mixture is therefore stirred for additional 2 h at 0 °C. The solution temperature is slowly raised to room temperature (25 °C) and the mixture is stirred for 30 h at room temperature to complete the reaction. The crude solid brown colored product comes out of the reaction mixture and is collected by centrifugation. The pure product is collected after repeated washing with methanol (to remove the impurities of unreacted silane, amine and amine-HCl salt) followed by vacuum drying at 60 °C for 24 h.

2.2.2. Transesterification reaction of alkoxy silane (Scheme 2)

To the degassed-dry ethanolic suspension of fullerenol (50 mg, 0.054 mM), alkoxy silane (3.24 mM) is added under argon atmosphere. The reaction mixture is refluxed for 30 h to complete the reaction. Solvent is removed under vacuum and the crude brown colored solid product (**4a** and **5a**) is washed several times with methanol to remove the impurity of silane.

3. Identification of the products

All the reactions have good reproducibility. The fullerenol–silane adducts (**1a**–**5a**) are brown-solid powdered material with high solubility in DMSO. Products are soluble in other solvents too (Section 5). The chemical attachment of silanes to fullerenol is easily monitored from the disappearance of typical fullerenol FT-IR peaks at 1593, 1381, and 1068 cm^{-1}. The general characteristic feature in displacement reaction will be the disappearance of Si–Cl (ν) (below 666 cm^{-1}) and the appearance of Si–O (ν) absorption peak at 1120 cm^{-1} in the FT-IR spectra of the products owing to the displacement of the chloride of chlorosilane with the hydroxyl group of fullerenol. The other peaks of silane, viz., ~3040 (ν, =C–H phenyl or alkene), 2960, 2870 (alkyl C–H) and 1630 (ν, C=C) cm^{-1} should be retained in the product also. In addition, the alcoholic C–O (ν) peak of fullerenol should be shifted due to the formation of new fol–O–Si linkage.

The representative FT-IR spectrum of the product **1a** (Fig. 1) shows the peaks at 3047 (ν, aromatic =C–H), 2960 (ν, C–H), 1603, 1590 (ν, aromatic C=C), 1427, 1380 (δ, CH_3), 1129 (ν, Si–O),

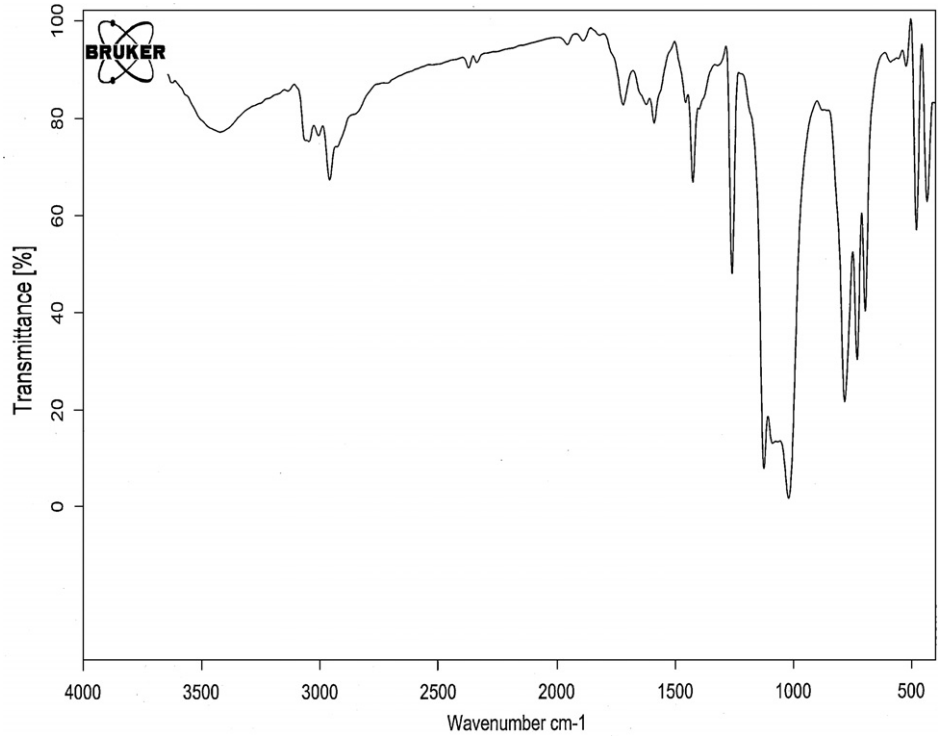

Fig. 1. FT-IR spectra of **1a** showing the aromatic and Si–O absorption peaks at 3047 and 1129 cm^{-1}, respectively.

1020 (ν, C–O–/δ, –OH), 697 (ν, Si–C). The occurrence of chemical reaction is characterized from the disappearance of characteristic fullerenol peaks at 1593, 1381 and 1068 cm^{-1}. The appearance of Si–O absorption peak at 1129 cm^{-1} (ν) and retention of aromatic absorption peaks at 3047 and 1590, 1480 cm^{-1} (ν, =C–H and C=C, respectively) in the product substantiate the proposed attachment of silane moiety to the fullerene core via displacement reaction. Shifting of C–O (ν) peak of fullerenol (1068–1020 cm^{-1}) in the product provide valuable input to understand the nucleophilic property of hydroxyl group of fullerenol to form fol–O–Si bond. The methyl C–H stretching and bending peaks at 2960, 2870 and 1427, 1380 cm^{-1} are retained in the product at their expected positions. Similar pattern are also observed in the FT-IR spectra of methyl/dimethylvinyl silane-fullerenol adducts (**2a** and **3a**). Si–O absorption peak is clearly observed in both the products (supporting information).

The FT-IR spectra of the transesterification reaction products also provide information for the disappearance of characteristic fullerenol peaks and support the chemical attachment of alkoxy silane moiety to the fullerene core. The peak to peak comparison of silane-fullerenol adducts and pure silane helps to gather more useful information. The silanes **4** shows the main FT-IR peaks at 3059, 2947, 2842, 1599, 1462, 1410, 1193, 1088, 1012, 969, 817, 772 cm^{-1} (Fig. 2A). The products **4a** retain most of the characteristic alkoxy silane peaks and show the main FT-IR absorption peaks at 3418 (ν, O–H), 3063 (ν, =C–H), 2959 and 2870 (ν, C–H), 1603 (ν, C=C), 1410 (δ, CH_3), 1136 (ν, Si–O), 1049 (ν, C–O–/δ, –OH), 967 (δ, =C–H, out of plane) and 810 (δ, $=CH_2$ wagging) cm^{-1} (Fig. 2B). Double bond peaks are retained in **4a**. Alkyl stretching and bending peaks are clearly visible and the shift in Si–O-stretching absorption suggests the change from Si–O–CH_3 to Si–O–fol. Compound **5a** also retains double bond and aromatic peaks (supporting information). The appearance of a broad peak at 3200–3400 cm^{-1} in all the products is due to the physically absorbed solvent molecules (observed in NMR and TGA analyses also).

The ^1H and ^{13}C NMR spectra of the products are recorded in DMSO using TMS as internal standard. The attachment of methylphenylsilane moiety to the fullerene core in **1a** is evident from the appearance of methyl proton peaks at δ 1.1 and aromatic protons at 7.1–7.3 ppm (Fig. 3A). The downfield shifting of the methyl peak (the methyl proton peak in dichloro methyl phenyl silane appears at 0.66 ppm) is due to the attachment of highly electronegative fullerene moiety. ^{13}C NMR spectrum (Fig. 3B) shows peak at 46.16 for CH_3 and six peaks between 127 and 136 for the six carbons

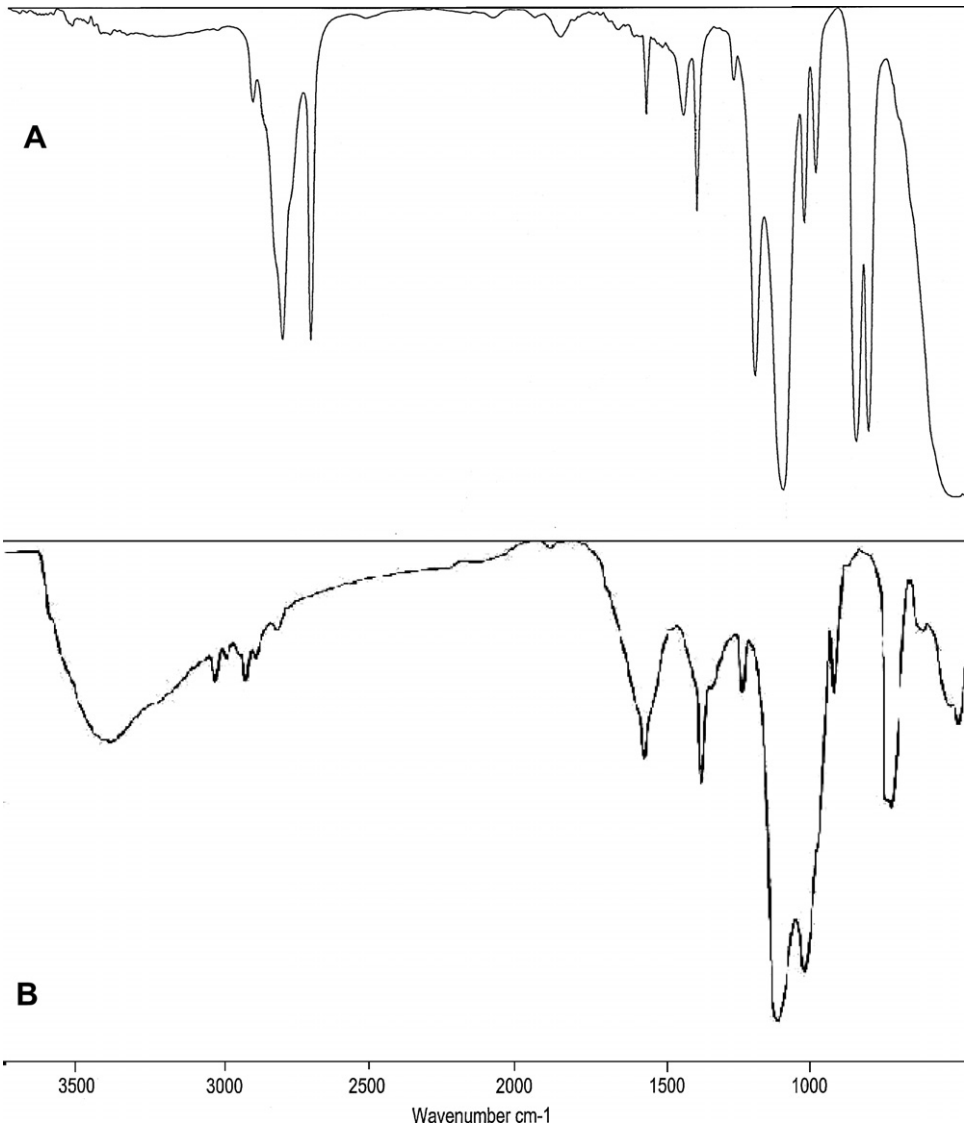

Fig. 2. FT-IR spectra of: (A) **4** and (B) **4a**.

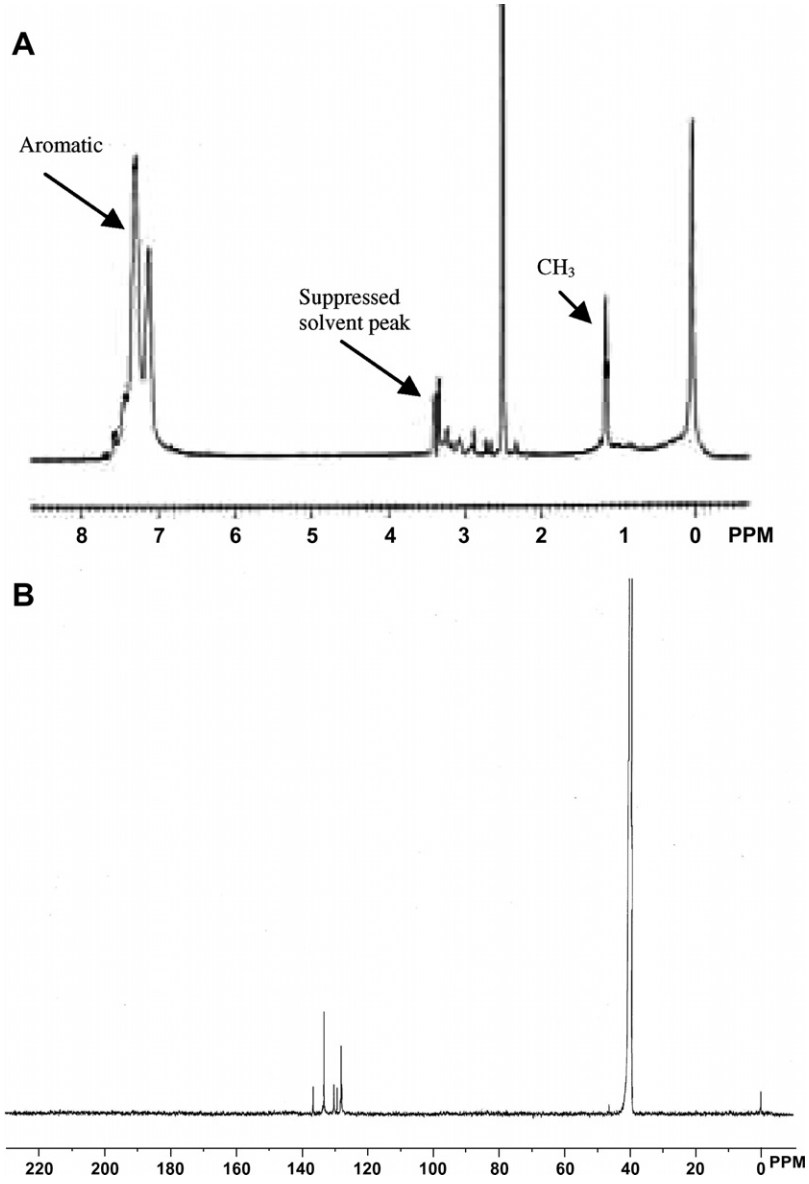

Fig. 3. (A) ^{1}H and (B) ^{13}C NMR spectra of **1a**.

of phenyl ring. Six different peaks of the phenyl carbons are possibly due to magnetically un-equivalent orientation of the molecule in three dimensions.

The methylvinyl silane-fullerenol adduct (**2a**) shows methyl peaks at 1.1 ppm and the vinylic proton peaks at 7.1–7.6 ppm in ^{1}H NMR. ^{13}C NMR spectrum, on the other hand, records peaks at δ 9.7 (CH_3), 79.52 (sp^3 hybridized fullerene carbons) and 128–132 for sp^2 fullerene carbons, respectively. Similarly adduct (**3a**) shows the proton peaks at δ 1.25 (6H, CH_3), 6.26–6.66 and 7.72 (dd, 3H, vinylic protons) in the ^{1}H NMR spectrum (supporting information). The presence of solvent impurity is indicated in the ^{1}H and ^{13}C NMR.

The ^{1}H NMR of vinyl silane-fullerenol adduct (**4a**) is also recorded in DMSO using TMS as internal standard. The spectrum (Fig. 4A) shows singlet methoxy proton peak at 3.78 ppm and the vinylic proton peaks at 7.18 and 7.26 ppm, respectively. The ^{13}C NMR spectrum (Fig. 4B) shows peaks at δ 66.72 (–O–CH_3), 125.68–129.27 (sp^2 hybridized carbon). The ^{1}H NMR spectra of the precursor material **5** and the product **5a** show the peaks at δ 3.36 (–O–CH_3–), 5.94–6.36 (–CH=CH_2) and 7.39–7.9 (naphthyl) and 5.8–6.3 (–CH=CH_2) and 7.39–7.9 (aromatic) ppm, respectively. The ^{13}C NMR spectra shows =CH_2 peak at 145.39 and other sp^2 hybridized peaks of fullerene between 122 and 165 ppm (supporting information).

Controlled mono-methoxy group participation in transesterification reaction is reasonably worked out by comparing the NMR spectra of **4a** and **5a**. Thus the spectrum shows a singlet methoxy at 3.78 for **4a** whereas methoxy peak is disappeared in **5a**. ^{13}C NMR also corroborates the ^{1}H NMR results. The methoxy peak appears at 66.72 ppm in **4a** and is absent in **5a**.

3.1. Mass analysis

The observed molecular ion peak in ESI-MS/FAB-MS of the fullerenol-alkoxy silane/chlorosilane adducts indicate the attachment of equal number of silane addends to that of initial hydroxyl groups. Representative ESI-MS spectrum of **4a** recorded in water is presented in Fig. 5. Molecular ion (M^+) peak at m/z 2228 indicate

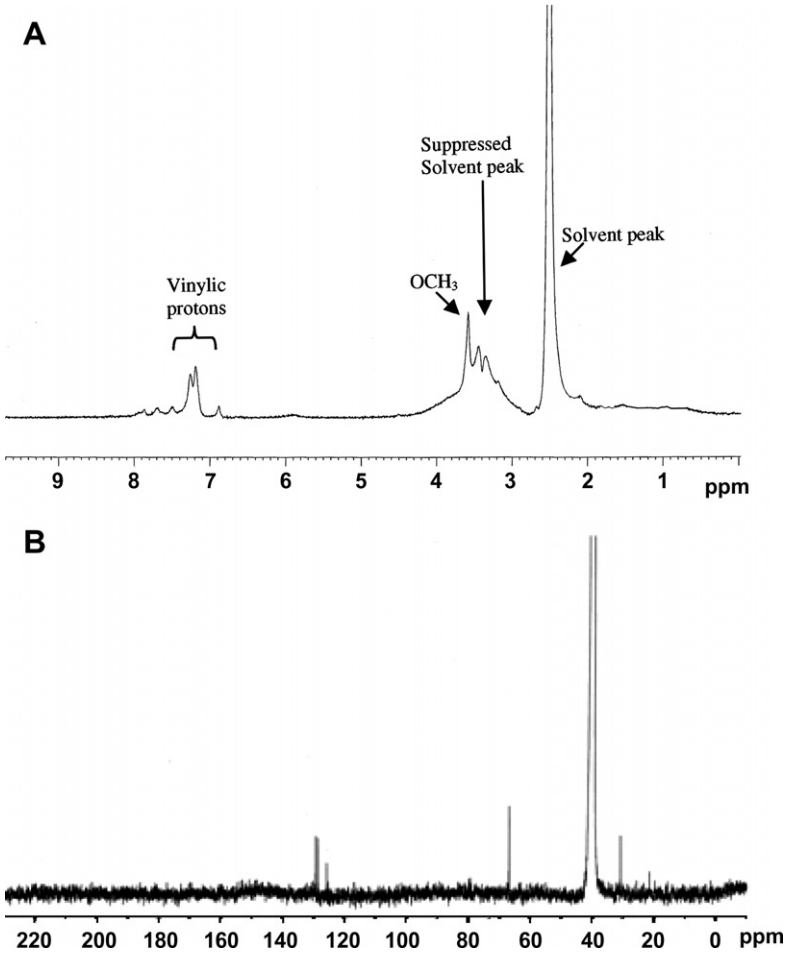

Fig. 4. (A) ^{1}H and (B) ^{13}C NMR spectra of **4a**.

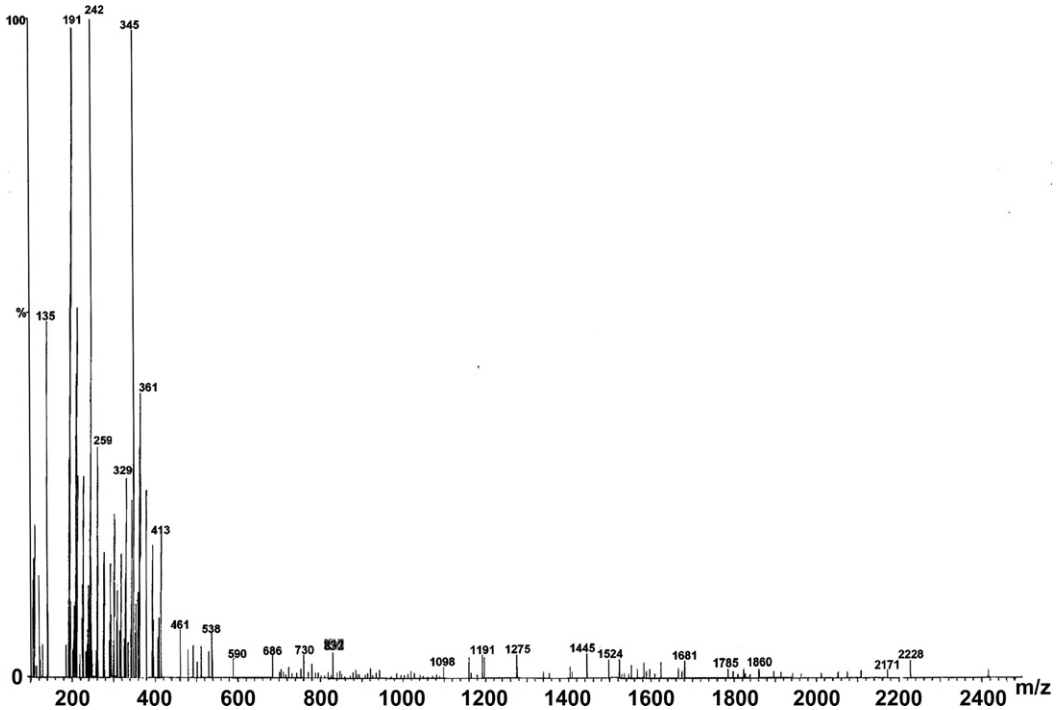

Fig. 5. ESI-MS of **4a** recorded in water.

the attachment of 14 alkoxy silane units (–O–Si–$(OH)_2$–CH_2=CH_2; with mass 105; the unreacted alkoxy group has undergone hydrolysis with water) [36] onto a single fullerene core. Other significant peaks that appear in the mass spectrum are at *m*/*z* (%) 2171 (2, C_{60} + 14 units – OH), 1860 (2, C_{60} + 11 units – OH), 1785 (2, C_{60} + 10 units + OH), 1681 (2, C_{60} + 9 units + OH), 1524 (2, C_{60} + 8 units – 2OH), 1275 (2, C_{60} + 5 units + 2OH), 1191 (2, C_{60} + 4 units + 3OH), 929 (2, C_{60} + 2 units), 912 (2, C_{60} + 2 units – OH).

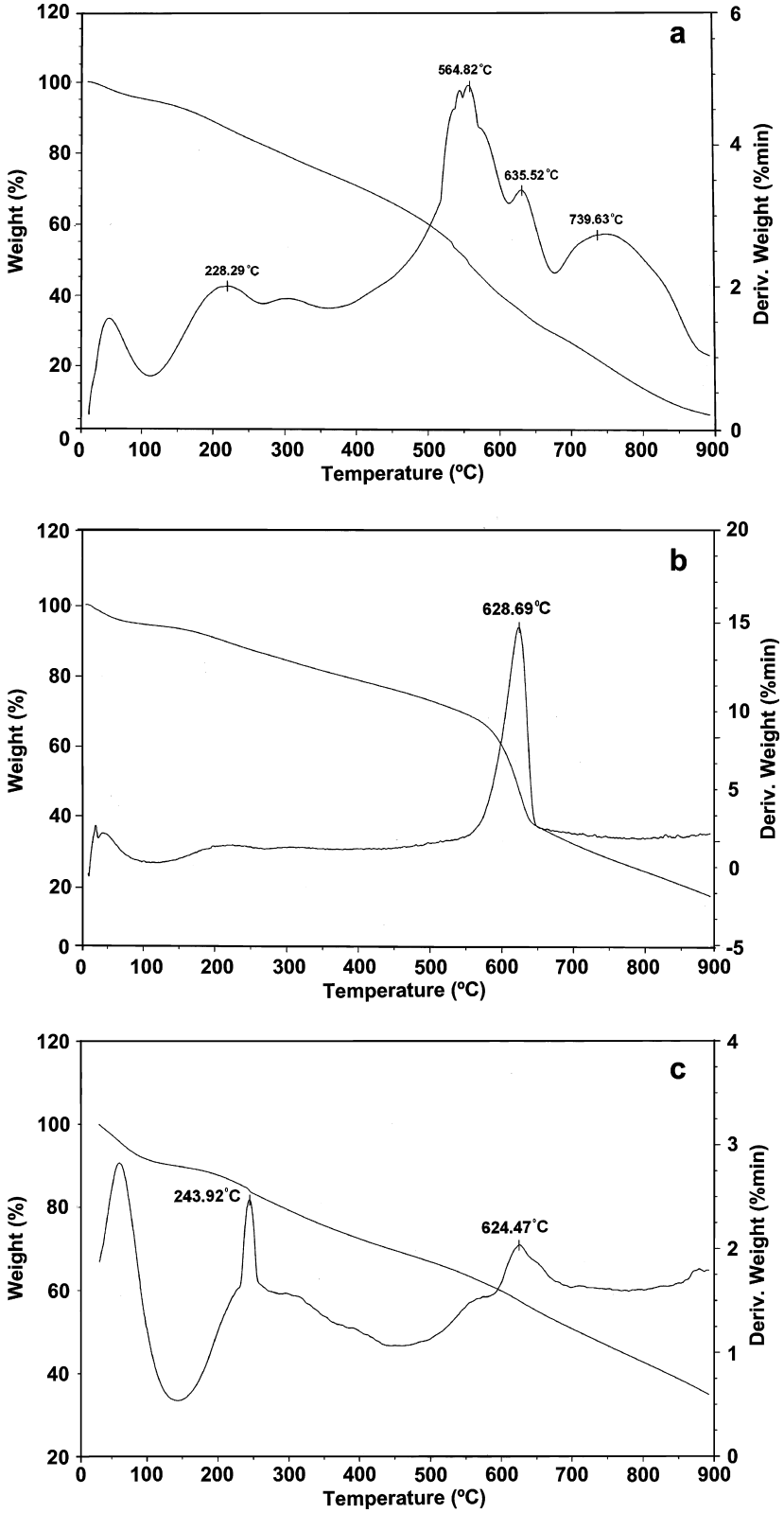

Fig. 6A. TGA and first derivative of: (a) **1a**, (b) **2a** and (c) **3a** recorded at a heating rate of 10 °C/min under N2 atmosphere.

3.2. Thermal analysis

TGA thermogram and the first derivative TGA trace of fullerenol–silane adducts and their comparison with unreacted fullerenol reveal several interesting observations. The analyses of thermal results help to ascertain the chemical attachment of silane moiety onto the fullerene core and also to predict their thermo-chemical behavior. Silicon has excellent thermal stability and chemical attachment of silicon into fullerene core is expected to enhance the thermal stability in fullerenol–silane adducts. The typical TGA thermogram and first derivative TGA traces of fullerenol and fullerenol–silane adducts (**1a**–**5a**, heating rate 10 °C/min in N_2 atm.) is depicted in Figs. 6A and 6B. The thermal data are summarized in Table 1. The initial weight loss and the associated degradation steps below 100 °C in all the samples is due to the removal of low boiling units inherently present in the samples. This observation ensures the presence physically absorbed solvent molecules in the products and complements the spectroscopic data.

The different nature of the thermogram of adducts compared to fullerenol is primarily due to the chemical attachment of silanes onto fullerene core. Substantial improvement of the thermal stability of adducts is apparent from conspicuous absence of usual degradation steps of the addends and shifting of the structural degradation step for fullerene moiety towards higher temperature zone. Although the TGA-thermogram follow a monotonic weight loss in the temperature range 150–570 °C, the first derivative does not show any prominent degradation step in many of the products. Instead it merges with structural degradation step of fullerene. A significant weight loss step is observed in **1a**, **3a** and **4a** in the temperature range of 200–300 °C. This step is quite insignificant in **5a** and is completely missing in **2a**. In these cases (**2a** and **5a**), the degradation at higher temperature appears as a single step with crest temperature at 629 and 785 °C, respectively. Interestingly, these steps are more prominent in sample where vinyl unit is absent. Moreover, char yield of these adducts are substantially higher (20% or more). Additional degradation step is also observed in **1a**. Thus incorporation of silicon into fullerene core produce thermally stable adducts.

3.3. UV–Vis analysis

The UV–Vis spectra of the products (**2a**, **3a** and **5a**) gives very little structural information's due to solubility problem. The strong possibility of aggregate formation in DMSO and water suppress the structured absorption peaks in UV-region. Thus the spectra recorded in DMSO show structureless absorption in UV region and extended tailing in the visible region characteristic of fullerene containing compounds [61]. Absorption spectrum of **4a** recorded in water (Fig. 7A) also shows similar structureless absorption in the UV region with extended tailing in the visible region. However

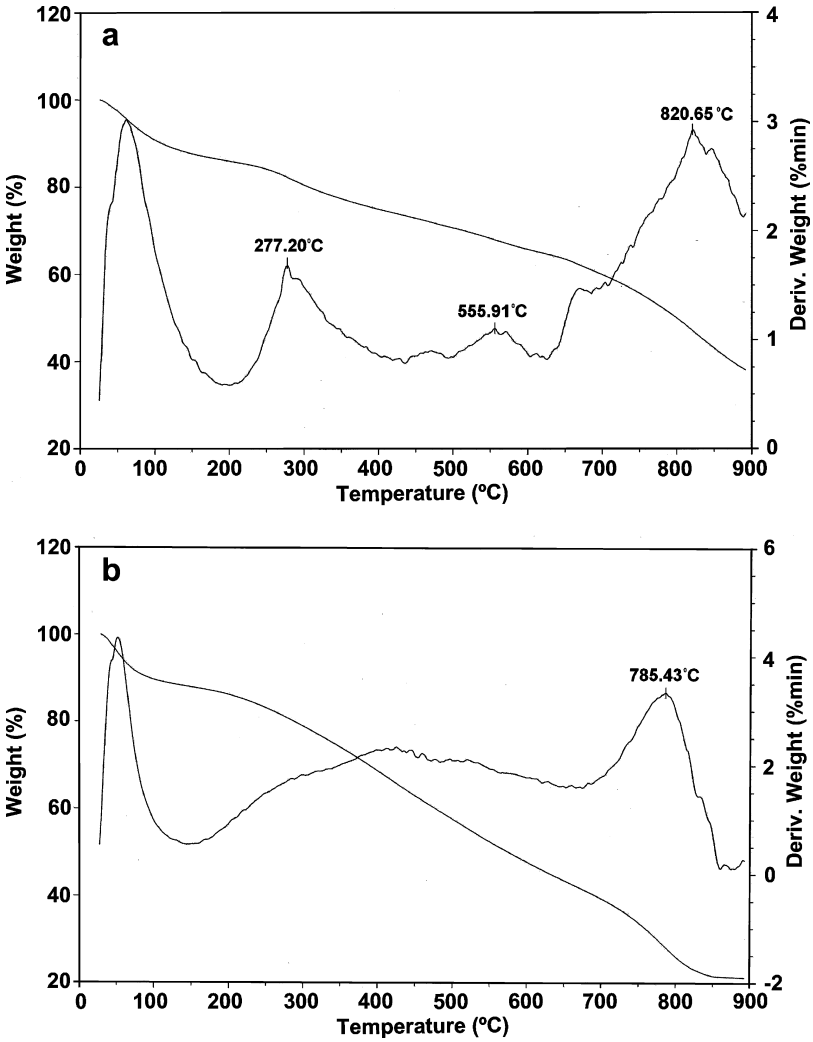

Fig. 6B. TGA and first derivative of: (a) **4a** and (b) **5a** recorded at a heating rate of 10 °C/min under N2 atmosphere.

Table 1
TGA results of product (**1a**–**5a**)

Product	Degradation		Crest temperature (°C)
	Temperature range (°C)	% wt loss	
Fullereol	150–570	24.41	214
1a	150–650	68.84	22856
2a	150–650	58.46	230629
3a	150–650	32.49	244624
4a	150–650	23.12	27755
5a	150–650	20.62	150650/785

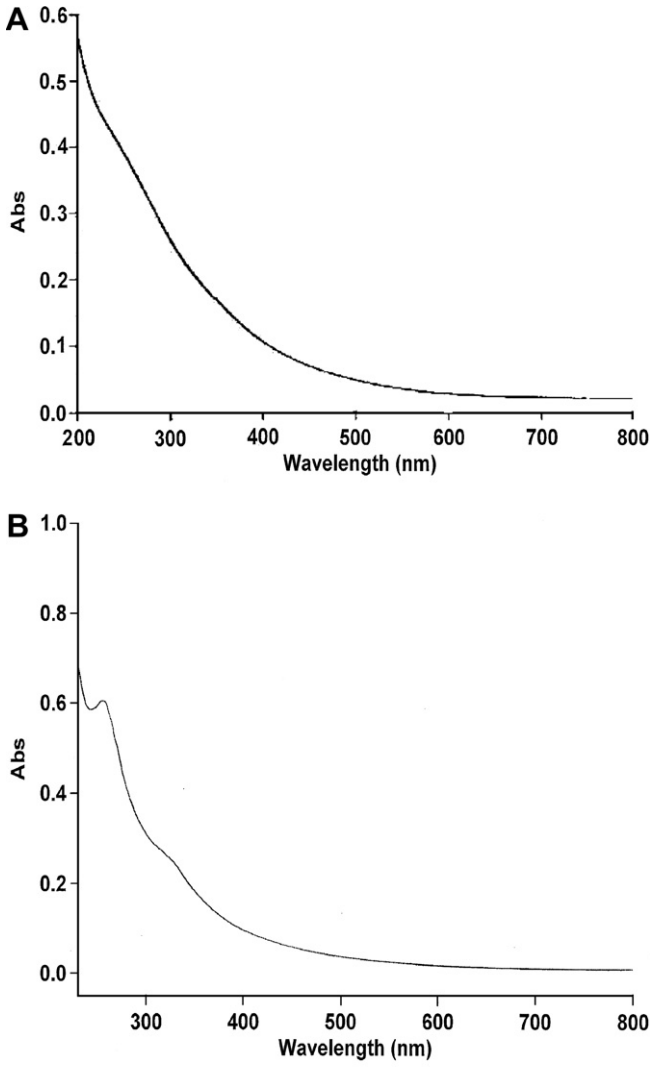

Fig. 7. UV–Vis spectra of (A) **4a** recorded in water and (B) **1a** recorded in DCM.

the UV–Vis spectrum of **1a** recorded in dichloromethane (Fig. 7B) gives structured absorption bands in UV region at 256 and 320 nm, respectively. The extended absorption of the phenyl ring is due to the π–π electronic interaction with fullerene core.

3.4. Photophysical properties

The characteristic photoluminescence (PL) emission spectra of fullerenol–silane adducts are recorded at room temperature in solid state using 350 nm excitation wavelength (λ_{ex} = 350 nm). Fullerenol shows a weak emission peak at 416 nm (3.00 eV)

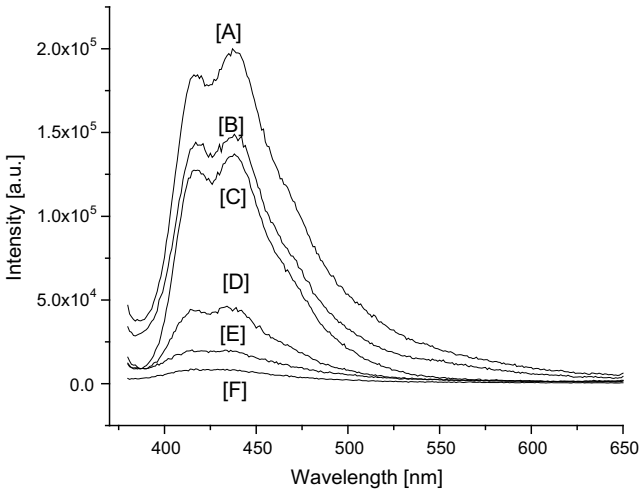

Fig. 8. Comparative fluorescence spectra of: (A) **3a**, (B) **2a**, (C) Fol, (D) **4a**, (E) **5a** and (F) **1a**.

followed by a strong shoulder peak at 437 nm (2.85 eV). The silane-fullerenol adducts also exhibit similar emission spectral profile to that of fullerenol. Fig. 8 and Table 2 apprise the comparative emission spectral profile of different silane-fullerenol adducts. The first weak emission energy peak (3.00 eV) of the functionalized fullerenol is due to the relaxation of photoexcited exciton or exciton–polaron from the upper vibrational level (S_12) of the lowest excited singlet state (t_1u) to the lowest state (h_u), which is usually symmetry forbidden one [62,63], forming a non-mobile negative polaron in C_{60} [64]. The strong shoulder emission peak (2.85 eV) shows that the primary emission occurs from the lower vibrational level (S_11) of the lowest excited singlet state (t_{1u}) to the lowest state (h_u) [62]. Controlled low-level functionalization restrict the perturbation of fullerene's symmetric π-electronic system in great deal. As a consequence, the energy difference between the first excited singlet (S_1) and lowest state (h_u) [65] in the functionalized-fullerene does not differ appreciably compared to pristine fullerenol and products are showing emission peaks approximately at the same position. However, the interaction between C_{60} and the addends make t_{1u}–h_u transition an allowed one due to interaction-induced cancellation of symmetry restrictions [64].

The luminescence intensity is significantly quenched in **1a**, **4a** and **5a**, with **1a** showing the highest quenching. Compounds **2a** and **3a**, on the other hand, show higher luminescence intensity compared to fullerenol. The most acceptable interpretation for the quenching could be the covalently attached photo-active aromatic units (π-donor groups) to fullerene core through short and flexible spacer creating a strong possibility for π–π electronic interaction. The formation of strong charge transfer (CT) exciplex between donor (aromatic ring) and acceptor (fullerene) and dissociation of photoexcited exciton or exciton–polaron (Ex–P) upon collision with C_{60} in nanosecond scale causes the quenching of PL intensity [66,67]. The results also suggest that the highest π–π interaction occurs between phenyl group and fullerene core and reduce with further delocalization of aromatic π-electrons in naphthalene. The increased electron population density in excited state

Table 2
PL emission peaks of different fullerenol–silane compounds (**1a**–**5a**)

Product	1a	2a	3a	4a	5a
Emission peak (nm/eV)	415/3.00 433/2.88	417/2.99 437/2.85	416/3.00 437/2.85	415/3.00 435/2.87	415/3.00 434/2.87

(+I effect of methyl) and ineffective charge transfer exciplex formation capability of isolated vinylic units may be a plausible reason of enhanced fluorescence intensity in adducts **2a** and **3a**.

3.5. Magnetic properties

EPR spectra recorded in solid state suggest that all the fullerenol–silane adducts (**1a**–**5a**) are paramagnetic in nature giving sharp signal at around 3515 G at room temperature. The covalent attachment of electropositive silicon and electronegative fullerene in shorter distance produce strong magnetic dipole moment on absorption of electromagnetic radiation of correct frequency in microwave region. The representative EPR spectrum of adduct **1a** is presented in Fig. 9A and EPR data of the derivatives are summarized in Table 3. Functionalized fullerenol **1a** shows strong and sharp signal at 3517.4 G with narrow line width and *g*-value 2.005. The peak to peak width (ΔH_{pp}) is 43 G and transverse spin–spin relaxation time ($T_2 = 1.31 \times 10^{-8}/g.\ \Delta H_{pp}$) is 0.1519×10^{-9} s. The pure fullerenol produces a similar EPR signal at 3520 G with $g = 1.985$ and a narrow line width with $\Delta H_{pp} = 12.5$ G ($T_2 = 5.27 \times 10^{-9}$ s). The higher peak width compared to pure fullerenol in all the samples (varying from 35 to 46 G) is due to the shorter lifetime of excited states and the molecule is readily relaxed back to ground state by transferring energy to other electron spin by spin–spin relaxation (T_2). T_2 value is of the order of nanoseconds in all the samples except **3a** where the spin–spin relaxation is of the order of picoseconds with very high peak width ($\Delta H_{pp} = 3157$ G). All the samples are showing higher *g*-value (2.005–2.007) compared to free electron ($g_e = 2.003$). The higher shift in *g* compared to g_e is due to partial contribution of the orbital angular momentum of Si involved in spin–orbit coupling. The sharp EPR signals observed in fullerenol and its silicon adducts are associated the removal of high symmetry of t_{1u} degeneracy and its Jahn-Teller distortion of pristine fullerene on functionalization [68]. The ESR spectrum of **3a** (Fig. 9B), however, is showing both broad and sharp signals possibly due to different saturation characteristic with applied microwave power. Among the various reasons reported earlier for the existence of such 'spike' signals, the presence of traces amount of impurity is most likely and is not ruled out in the present case [68]. The pin point characterization and its quantification by conventional spectroscopic methods are, however, very difficult to obtain for this type of impurities.

Table 3
EPR data for silane–fullerenol adducts

Product	ΔH_{pp} (G)	*g*-Value	T_2 (s)
1a	47	2.005	0.15193×10^{-9}
2a	36	2.005	0.18153×10^{-9}
3a	3157	2.009	2.0653×10^{-12}
4a	46	2.007	0.14193×10^{-9}
5a	35	2.0055	0.1863×10^{-9}

4. Conclusion

The organosilane–fullerenol adducts are easily accessible through transesterification and displacement reactions. The thermal and fluorescence properties of fullerenol are considerably influenced due to the presence of organosilicon moiety in the functionalized fullerenol. The stable charge-transfer exciplex is formed with the silanes having closed π-conjugated system and considerably quench the fluorescence intensity due to π–π electronic interactions between aromatic system (donor) and fullerene core (acceptor). On the contrary, alkyl-vinyl silane adducts show enhanced fluorescence intensity compared to unreacted fullerenol. Also, these adduct exhibit strong paramagnetic properties in solid state at room temperature. These compounds may find promising applications in opto-electronic and opto-magnetic devices and magnetic recording systems. The presence of free vinylic moiety also promises chemical manipulation to synthesize fullerene containing organo-silicon polymers.

5. Experimental

5.1. Materials

[60]Fullerene is obtained from MER Co. (purity > 99.5%). The sample quality is checked by UV/Vis absorption, ^{13}C NMR, and is used without further purification. Dichloro phenyl methyl silane (**1**), dichloromethyl vinylsilane (**2**), monochlorodimethyl vinyl silane (**3**) and trimethoxy vinyl silane (**4**) are purchased from Lancaster and used as received. Dinaphthyl methoxy vinyl silane (**5**) is prepared in laboratory. DMF is dried over calcium hydride and distilled under vacuum before experiment. Tri ethylamine is kept over KOH and freshly distilled before use.

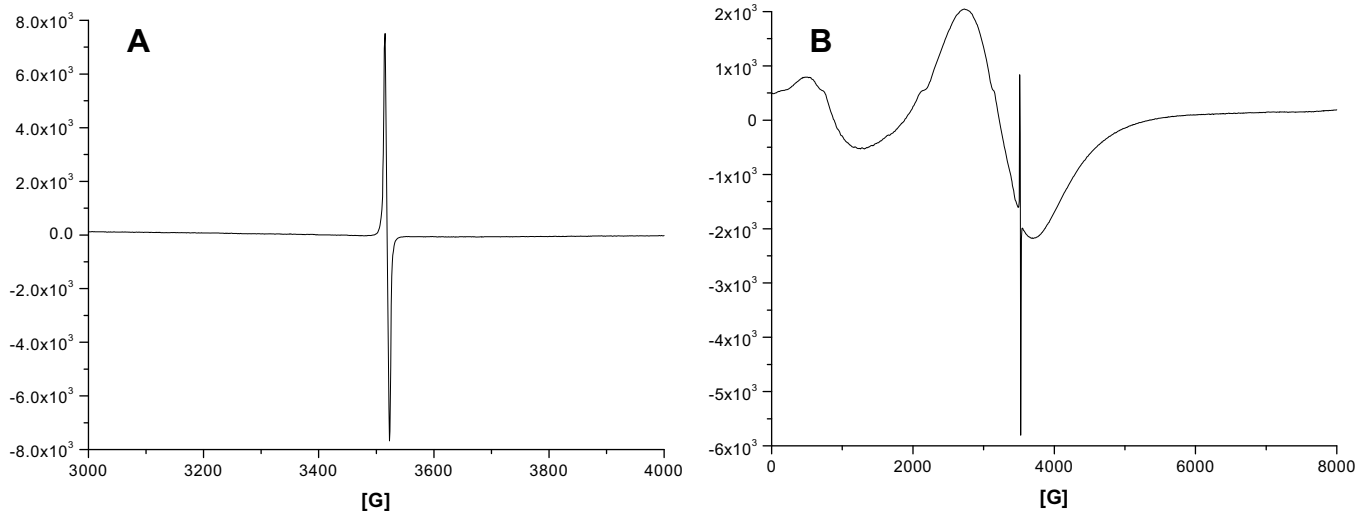

Fig. 9. Representative EPR spectra of: (A) **1a** and (B) **3a** recorded in solid state.

5.2. Preparation of **1a**

Fullerenol (0.05 g, 0.052 mM) is suspended in dry DMF (20 mL) and degassed with argon. Triethyl amine is added in excess (10 mL) and silane **1** (3.24 mM) is added very slowly in ice-cooled condition. After complete addition the temperature is maintained at 0 °C for further 2 h and then slowly rose to room temperature. Stirring is continued at room temperature under inert atmosphere for 30 h. Diethyl ether is added under ice cooled condition for complete precipitation of the product. Brown colored solid product is collected by centrifugation and is washed several times with methanol to remove the impurity of triethyl amine-HCl salt and unreacted silane (yield = 37 mg; 74%). Solubility: DMSO, MeOH, $CHCl_3$, DCM. FT-IR (KBr, cm^{-1}): 3047 (ν, aromatic =C–H), 2960 (ν, C–H), 1603, 1590 (ν, aromatic C=C), 1427, 1380 (δ, CH_3), 1129 (ν, Si–O), 1020 (ν, C–O–/δ, –OH), 697 (ν, Si–C); ^{1}H NMR (DMSO, δ): 1.1 (3H, CH_3), 7.1–7.3 (s, 6H, CH_3); ^{13}C NMR 40.1 (CH_3), 127–136 (six peaks for phenyl carbons).

5.3. Preparation of **2a**

Synthesis method applied as above using silane **2** (3.24 mM) in excess (yield = 28 mg; 56%). Solubility: DMSO. FT-IR (KBr, cm^{-1}): 3030 (ν, =C–H), 2970 and 2931 (ν, C–H), 1630 (ν, C=C), 1450 and 1386 (δ, CH_3), 1098 (ν, Si–O), 1020 (ν, C–O–/δ, –OH); FTNMR (^{1}H and ^{13}C, DMSO, δ): 1.1 (CH_3), 7.1–7.6 (vinylic protons) and 9.7 (CH_3), 79.52 (sp^3 hybridized fullerene carbons), 128–132 (sp^2 hybridized carbons). FAB-MS (DMSO, m/z): 2311 [C_{60} + 16 units – 2CH=CH_2], 2094 [C_{60} + 13 units + 2OH], 1992 [C_{60} + 12 units + 2OH], 1934 [C_{60} + 11 units + 5OH], 1786 [C_{60} + 10 units + 2OH], 1765 [C_{60} + 10 units + OH], 1518 [C_{60} + 8 units – CH=CH_2], 1441 [C_{60} + 7 units], 1407 [C_{60} + 6 units + 4OH], 1205 [C_{60} + 5 units – CH_3–OH], 1147 [C_{60} + 4 units + O], 1045 [C_{60} + 3 units + O], 906 [C_{60} + 1 units + 5OH].

5.4. Preparation of **3a**

Product III is synthesized applying the same procedure as above using silane **3** (yield = 21 mg; 42%). Solubility: DMSO. FT-IR (KBr, cm^{-1}): 3000 (ν, =C–H), 2970 and 2931 (ν, C–H), 1630 (ν, C=C), 1473 and 1386 (δ, CH_3), 1100 (ν, Si–O), 1060 (ν, C–O–/δ, –OH), 630 (ν, Si–C); FTNMR (DMSO, δ): 1.25 (CH_3), 6.6 (=CH_2), 7.7 (–CH=). FAB-MS (DMSO, m/z): 2084 [C_{60} + 13units + 3OH], 2004 [C_{60} + 13units – CH=CH_2], 1907 [C_{60} + 12units – CH=CH_2], 1866 [C_{60} + 11units + 2OH], 1787 [C_{60} + 10units + 3OH], 1666 [C_{60} + 9units + 2OH], 1517 [C_{60} + 7units + 5OH], 1459 [C_{60} + 7units + 2OH], 1259 [C_{60} + 5units + 2OH], 1094 [C_{60} + 3units + 4OH].

5.5. Preparation of **4a**

To the degas ethanolic suspension of fullerenol (0.05 g, 0.052 mM in 30 mL), trimethoxy vinyl silane **4** (3.24 mM) is added slowly and refluxed at 70 °C for 30 h. Solvent is evaporated by vacuum drying and washes several times with methanol (yield = 30 mg; 60%). Solubility: DMSO, water. FT-IR (KBr, cm^{-1}): 3418 (ν, O–H), 3063 (ν, =C–H), 2959 and 2870 (ν, C–H), 1603 (ν, C=C), 1410 (δ, CH_3), 1136 (ν, Si–O), 1049 (ν, C–O–/δ, –OH), 967 (δ, =C–H, out of plane) and 810 (δ, =CH_2 wagging); FTNMR (^{1}H ^{13}C and DMSO, δ): 3.78 (–O–CH_3), 7.18 and 7.26 (vinylic protons) and 66.72 (–O–CH_3), 125.68–129.27 (sp^2 hybridized carbon).

5.6. Preparation of **5a**. Synthesis of **5**

Grignard reagent of 1-bromo naphthalene is prepares by reaction of 1-bromo naphthalene (0.050 mM) with magnesium (0.052 mM) in dry THF at 0 °C. The reagent is transferred to the THF solution of trimethoxy vinyl silane (0.5 mM). Reaction mixture is refluxed at 70 °C for 70 h, then filtered and rota-evaporated. The product was portioned by fractional distillation. FT-IR (KBr, cm^{-1}): 3052, 2942, 2837, 1592, 1504, 1403, 1189, 1147, 1081, 1007, 962, 779, 692, 638, 552 and 475 cm^{-1}. ^{1}H NMR ($CDCl_3$, δ): 3.36 (s, 3H, –O–CH_3), 5.94–6.36 (–CH =CH_2).

5.7. Synthesis of **5a**

Procedure adopted same as **4a** using dinaphthyl methoxy vinyl silane (**5**) as the silylating agent (yield = 56%). Solubility: DMSO. FT-IR (KBr, cm^{-1}): 3392 (ν, O–H), broadening containing peaks of aromatic =C–H (ν) and alkyl C–H (ν) at ~3050, 1598, 1400 (ν, C=C), broad peak at 1120 and 1072 for Si–O and C–O (ν); FTNMR (^{1}H, DMSO, δ): 5.8–6.3 (–CH=CH_2), 7.39–7.9 (m, aromatic protons).

6. Characterization

FT-IR spectra are recorded on a Nicolet Magna IR 750 Spectrometer, using KBr pellets. ^{1}H and ^{13}C NMR spectra are recorded on Bruker Av 400 spectrometer operating at frequency of 400 MHz in DMSO using TMS as the internal standard. The electrospray mass spectra (ESI-MS) are recorded on a MICROMASS QUATTRO II triple quadrupole mass spectrometer. Aqueous solution of the sample is introduced into the ESI source through a syringe pump at the rate of 5 μL per min. The ESI capillary is set at 3.5 kV and the cone voltage was 40 V. The spectra are collected in 6 s scans and the print outs are averaged spectra of 6–8 such scans. The FAB mass spectra are recorded on a JEOL SX 102/DA-6000 Mass Spectrometer/Data System using argon/xenon (6 kV, 10 mA) as the FAB gas. The accelerating voltage is 10 kV and the spectra are recorded at r.t., *m*-Nitrobenzyl alcohol (NBA) as matrix. Thermal properties are measured using a Hi-Res TGA 2950 Thermogravimetric Analyzer (TA Instruments) attached to a Thermal Analyst 2100 (Du Pont Instruments) thermal analyzer, at a heating rate of 10 °C/min under N_2 atmosphere. The UV–Vis spectra of the products are recorded on a Varian-CARY 500 UV–VIS–NIR spectrophotometer in DCM/DMSO/water at equal concentration using methanol (spectroscopy grade) as the standard reference. A commercial spectrofluorometer (SPEX, Fluorolog 3, Model FL 3–22) is used to record the fluorescence spectra. The excitation light from a 450 W xenon lamp having a spot size dimension of ~2 mm × 10 mm is incident on the solid sample kept in steel sample holder with a path length of 10 mm. The fluorescence spectra (λ_{EM} = 470–800 nm) from the samples are recorded with 350 nm excitation wavelength. All the spectra are collected at 22.5° from the direction of the incident excitation light to minimize the spectral reflection from the surface. The band-pass for both the excitation and emission monochromator is 2 nm. The integration time is kept 0.1 s and the emission monochromator stepped through 1 nm while recording spectra. EPR spectra are recorded on Brucker WINEPR spectrometer at room temperature (25 °C), and *g*-values are determined by calibrating to DPPH.

Acknowledgements

The authors sincerely acknowledge IIT-Kanpur and CDRI, Lucknow for recording PL, EPR and Mass, respectively. Thanks are also due to Ajit Srivastava, A.K. Pandey, Amitabh Chakravarty, A.K. Saxena and Pushpa Bhargava for recording NMR, UV–Vis, TGA and FT-IR. The authors hearty acknowledge Dr. Santosh K. Tripathi for useful scientific support.

Appendix A. Supplementary material

Supplementary data associated with this article can be found, in the online version, at doi:10.1016/j.jorganchem.2008.03.006.

References

[1] S.P. Chou, H. Kuo, C. Wang, C. Tsai, C. Sun, J. Org. Chem. 54 (1989) 868.
[2] (a) Y. Hatanaka, T. Hiyama, J. Org. Chem. 53 (1988) 918;
(b) Y. Hatanaka, T. Hiyama, J. Org. Chem. 54 (1989) 268.
[3] J. Hartmann, M. Schlosser, Helv. Chim. Acta 59 (1976) 453.
[4] C. Yuanyin, F. Pengfri, Z. Zhaorui, F. Jianhong, Chem. Lett. (1999) 499.
[5] A. Glausch, A. Hirsch, I. Lamparth, V. Schurig, Chromatography A 809 (1998) 252.
[6] B. Gross, V. Schurig, I. Lamparth, A. Hirsch, J. Chromatogr., Sect. A 79 (1997) 65.
[7] Y.Y. Chen, P.F. Fang, Z.R. Zeng, J.H. Fan, Chem. Lett. (1999) 495.
[8] P.F. Fang, Z.R. Zeng, J.H. Fan, Y.Y. Chen, Chromatography A 867 (1999) 177.
[9] X. Li, Y. Chen, P. Fang, S. Gong, Ind. J. Chem. 42B (2003) 1111.
[10] M. Maggini, C. De Faveri, G. Scorrano, M. Prato, G. Brusatin, M. Guglielmi, M. Meneghetti, R. Signorini, R. Bozio, Chem. Eur. J. 5 (1999) 2501.
[11] A. Bianco, F. Gasparrini, M. Maggini, D. Misiti, A. Polese, M. Prato, G. Scorrano, C. Toniolo, C. Villani, J. Am. Chem. Soc. 119 (1997) 7550.
[12] R. Signoroni, S. Sartori, M. Meneghetti, R. Bozio, M. Maggini, G. Scorrano, M. Prato, G. Brusatin, M. Guglielmi, Mol. Cryst. Liq. Cryst., Sect B, Nonlin. Opt. 21 (1999) 143.
[13] R. Signoroni, M. Meneghetti, R. Bozio, M. Maggini, G. Scorrano, M. Prato, G. Brusatin, M. Guglielmi, G. Brusatin, P. Innocenzi, M. Guglielmi, Carbon 38 (2000) 1653.
[14] R. Signoroni, M. Meneghetti, R. Bozio, G. Brusatin, P. Innocenzi, M. Guglielmi, F. Della, J. Negra, J. Sol–Gel Sci. Technol. 22 (2001) 245.
[15] K. Kordatos, M. Prato, E. Menna, G. Scorrano, M. Maggini, J. Sol–Gel Sci. Technol. 22 (2001) 237.
[16] J. Schell, D. Felder, J.-F. Nierengarten, J.-L. Rehspringer, R. Levy, B. Hornelage, J. Sol–Gel Sci. Technol. 22 (2001) 225.
[17] G. Brusatin, R. Signorini, J. Mater. Chem. 12 (2002) 1964.
[18] Y. Rio, D. Felder, G. Kopitkovas, A. Churgreev, J.-F. Nierengarten, R. Levy, J.L. Rehspringer, J. Sol–Gel Sci. Technol. 26 (2003) 625.
[19] P. Innocenzi, B. Lebeau, J. Mater. Chem. 15 (2005) 3821.
[20] P. Belik, A. Gugel, J. Spickermann, K. Mullen, Angew. Chem., Int. Ed. Engl. 32 (1993) 90.
[21] A. Gugel, A. Kraus, J. Spickermann, P. Belik, K. Mullen, Angew. Chem., Int. Ed. Engl. 33 (1994) 559.
[22] P. Belik, A. Gugel, A. Kraus, J. Spickermann, K. Mullen, Adv. Mater. 5 (1993) 854.
[23] A. Kraus, A. Gugel, P. Belik, M. Walter, K. Mullen, Tetrahedron 51 (1995) 9927.
[24] L.J. Anderson, Y.Z. An, Y. Rubin, C.S. Foote, J. Am. Chem. Soc. 116 (1994) 1569.
[25] U.M. Fernandez-Panaigua, B. Illescas, N. Martin, C. Seoane, P. de la Cruz, A. de la Hoz, F. Langa, J. Org. Chem. 62 (1997) 3705.
[26] A. Kraus, K. Mullen, Macromolecules 32 (1999) 4214.
[27] M.L. Miller, R. West, Chem. Commun. (1999) 1797.
[28] T. Wakahara, Y. Maede, M. Kako, T. Akasaka, K. Kbayashi, S. Nagane, J. Organomet. Chem. 685 (2003) 177.
[29] M.E. Rincon, H. Hu, J. Campos, J. Ruiz-Garcia, J. Phys. Chem. B 107 (2003) 4111.
[30] Y.M. Li, K. Hinokuma, Solid States Ionics 150 (2002) 309.
[31] K. Hinokuma, M. Ata, Chem. Phys. Lett. 341 (2001) 442.
[32] J.D. He, J. Hang, S.D. Li, M.K. Cheung, J. Appl. Polym. Sci. 81 (2001) 1286.
[33] (a) S. Campidelli, J. Lenoble, J. Barbera, F. Paolucci, M. Marcaccio, D. Paolucci, R. Deschenaux, Macromolecules 38 (2005) 7915;
(b) W.-S. Li, K.S. Kim, D.-L. Jiang, H. Tanaka, T. Kawai, J.H. Kwon, D. Kim, T. Aida, J. Am. Chem. Soc. 128 (2006) 10527.
[34] T.D. Ros, M. Prato, Chem. Commun. (1999) 663.
[35] H. Kato, Y. Kanazawa, H. Okumura, A. Taninaka, T. Yokawa, H. Shinohare, J. Am. Chem. Soc. 125 (2003) 4391.
[36] M. Mikawa, H. Kato, M. Okumura, M. Narazaki, Y. Kanazawa, N. Miwa, H. Shinohara, Bioconjugate Chem. 12 (2001) 510.
[37] R.D. Bolsker, A.F. Benedetto, L.O. Husebo, R.E. Price, E.F. Jackson, S. Wallace, L.J. Wilson, J.M. Alford, J. Am. Chem. Soc. 125 (2003) 5471.
[38] K.L. Wooley, C.J. Hawker, J.M. Frechet, J. Am. Chem. Soc. 115 (1993) 9836.
[39] M. Kawaguchi, A. Ikeda, S. Shikai, J. Chem. Soc., Perkin Trans. 1 (1998) 179.
[40] C.J. Hawker, K.L. Wooley, J.M. Frechet, J. Am. Chem. Soc. (1994) 925.
[41] E. Koudoumas, M. Konstantaki, A. Mavromanolakis, S. Couris, Y. Ederle, C. Mathis, P. Seta, S. Leach, Chem. Phys. Lett. 335 (2001) 533.
[42] E. Cloutet, Y. Gnanou, J.-L. Fillaut, D. Astruc, Chem. Commun. (1996) 1565.
[43] Y. Chen, W.S. Huang, Z.E. Huang, R.F. Cai, S.M. Chen, X.M. Yen, Eur. Polym. J. 33 (1997) 823.
[44] L.Y. Wang, V. Ananthraj, K. Ashok, L.Y. Chiang, Synth. Met. 103 (1999) 2350.
[45] T. Zhang, K. Xi, X. Yu, S. Guo, B. Gu, H. Wang, Polymer 44 (2003) 2647.
[46] B. Yu, Y. Chen, R. Cai, Z. Huang, Y. Xiao, Eur. Polym. J. 33 (1999) 3049.
[47] T.H. Goswami, B. Nandan, S. Alam, G.N. Mathur, Polymer 44 (2003) 3209.
[48] T.H. Goswami, R. Singh, S. Alam, G.N. Mathur, Chem. Mater. 16 (2004) 2442.
[49] L.Y. Chiang, L.Y. Wang, S.M. Tseng, J.S. Wu, K.H. Hseih, J. Chem. Soc., Chem. Commun. (1994) 2675.
[50] L.Y. Chiang, L.Y. Wang, C.S. Kuo, Macromolecules 28 (1995) 7574.
[51] T. Song, S. Dai, K.C. Tam, S.Y. Lee, S.H. Goh, Polymer 44 (2003) 2529.
[52] T.H. Goswami, R. Singh, Synth. Met. 157 (2007) 951.
[53] T.H. Goswami, R. Singh, J. Phys. Org. Chem. 21 (2008) 225.
[54] T.H. Goswami, R. Singh, Schiff Base Mediated 1,2 Michael Addition Reactions of Fullerenol (communicated), 2008.
[55] M. Iglesias, A. Santos, J. Organomet. Chem. 553 (1998) 193.
[56] (a) S. Yamago, M. Yanagawa, E. Nakamura, J. Chem. Soc., Chem. Commun. (1994) 2093;
(b) S. Yamago, M. Yanagawa, H. Mukai, E. Nakamura, Tetrahedron 52 (1966) 5091.
[57] J. Ouyang, S.H. Goh, H.I. Elim, G.C. Meng, W. Ji, Chem. Phys. Lett. 366 (2002) 224.
[58] J. Ouyang, S. Zhou, F. Wang, S.H. Goh, J. Phys. Chem. B 108 (2004) 5937.
[59] J. Li, A. Takeuchi, M. Ozawa, X. Li, K. Saigo, K. Kitazawa, Chem. Commun. (1993) 1784.
[60] (a) T.H. Goswami, R. Singh, in: Carl N. Kramer (Ed.), Fullerene Research Advances, NOVA Science Publishers, NY, 2007, pp. 55–96 (Chapter 3) entitled "Recent Development of Fullerenol Chemistry" (ISBN: 1-60021-824-5). On reducing the concentration of NaOH to 100 times (2 g in 200 mL), the same reaction (Ref. [37]) can produce $C_{60}(OH)_{16-18}$, whereas reducing the amount of NaOH and time (0.15 g NaOH in 10 mL water, 2 h), the reaction yield $C_{60}(OH)_{12-14}$.;
(b) T.H. Goswami, R. Singh, S. Alam, G.N. Mathur, Thermochim. Acta 419 (2004) 97.
[61] L. Xiao, H. Shimotani, N. Dragoe, A. Sugita, K. Saigo, Y. Iwasa, T. Kobayashi, K. Kitazawa, Chem. Phys. Lett. 368 (2003) 738.
[62] S. Morita, S. Kiyomatsu, X.H. Yin, A.A. Zakhidov, T. Noguchi, T. Ohnishi, K. Yoshino, J. Appl. Phys. 74 (1993) 2860.
[63] J. Mort, K. Okumura, M. Machonkin, R. Ziolo, D.R. Huffmann, M.I. Feguson, Chem. Phys. Lett. 186 (1991) 281.
[64] D.M. Guldi, K.D. Asmus, J. Phys. Chem. A 101 (1997) 1472.
[65] (a) S. Morita, A.A. Zakhidov, K. Yoshino, Solid State Commun. 82 (1992) 249;
(b) K. Yoshino, S. Morita, T. Kawai, H. Araki, X.H. Yin, A.A. Zakhidov, Synth. Met. 56 (1993) 2991.
[66] R.B. Martin, K. Fu, H. Li, D. Cole, Y.P. Sun, Chem. Commun. (2003) 2368.
[67] K. Yoshino, X.H. Yin, K. Muro, S. Kiyomatsu, S. Morita, A.A. Zakhidov, T. Noguchi, T. Ohnishi, Jpn. J. Appl. Phys. 32 (1993) L357.
[68] (a) S.S. Eaton, G.R. Eaton, Appl. Magn. Reson. 11 (1996) 155;
(b) P. Boulas, R. Subramanian, W. Kutner, M.T. Jones, K.M. Kadish, J. Electrochem. Soc. 140 (1993) L130;
(c) C.A. Reed, R.D. Bolskar, Chem. Rev. 100 (2000) 1075. and references therein.